

39. ELEMENT STRATIGRAPHY ACROSS THE CRETACEOUS/TERTIARY BOUNDARY IN HOLE 738C¹

Birger Schmitz,² Frank Asaro,³ Helen V. Michel,³ Hans R. Thierstein,⁴ and Brian T. Huber⁵

ABSTRACT

Neutron activation analyses of iridium and other chemical elements were performed across a 1-m-thick, partly non-bioturbated, clay-rich interval at the Cretaceous/Tertiary boundary in ODP Hole 738C. The results show that the boundary interval holds one of the highest Ir enrichments (320 ng Ir/cm²) of all known Cretaceous/Tertiary boundary layers. Iridium concentrations are highest (18 ppb Ir, whole-rock samples) a few centimeters above the base of the clay-rich interval and gradually tail off upsection. Compared with background levels the most Ir-rich interval also shows strongly enhanced concentrations of Cr (215 ppm) and slightly elevated Co concentrations (13 ppm).

The Ir-rich interval shows low As (<15 ppm) and Sb (<0.8 ppm) concentrations, a fact that is congruent with absence of abundant authigenic sulfides in the sediment. Irregularly distributed Fe enrichments and a greenish gray color of the Fe-rich intervals may indicate the presence of glauconitic clay minerals and suboxic, slightly reducing conditions during deposition. Rare earth element (REE) abundance patterns change considerably across the Cretaceous/Tertiary boundary interval, reflecting either a change in Cretaceous/Tertiary boundary seawater REE composition or the occurrence of different REE fractionation processes due to changing depositional environment. Element-vs.-element ratios of Hf, Ta, Th, U, Cs, and Sc are similar between the most Ir-rich layers of the boundary section and other levels with lower Ir concentrations. This may imply that the clay fraction of the Ir-rich layers of the Cretaceous/Tertiary boundary interval is made up predominantly of locally derived material. Calculated calcite-free abundances of Hf, Ta, Th, U, Cs, and Sc, on the other hand, are reconcilable with an extraneous origin of the bulk of the clay in the most Ir-rich layers.

The Ir in the Cretaceous/Tertiary boundary clay-rich zone in Hole 738C is most likely derived from an earth-impacting asteroid; however, the origin of the clay-rich zone remains enigmatic.

INTRODUCTION

The upper Maestrichtian and lower Danian sediments in Ocean Drilling Program (ODP) Hole 738C are made up of pure limestones and chalks, and, like in many similar marine Cretaceous/Tertiary boundary sequences distributed worldwide, a clay-rich layer is found at the level where many of the Cretaceous phytoplankton and zooplankton species become extinct (e.g., Alvarez et al., 1980; Michel et al., 1983; Smit and Romein, 1985; Schmitz, 1988b). The basal 15 cm of this marl or clay-rich calcareous ooze is finely laminated, indicating the absence of bioturbation during deposition (Thierstein et al., this volume). This implies that the laminated interval may contain an extremely detailed microstratigraphic record of a possibly complex sequence of events causing trauma in the marine biosphere.

The shipboard scientific party asked us to study the distribution of chemical elements across the Cretaceous/Tertiary boundary in Hole 738C. Our major objective was to determine whether the boundary clay-rich zone is associated with an Ir anomaly and, if so, to localize this anomaly in relation to the boundary faunal and floral turnovers. Iridium anomalies at the Cretaceous/Tertiary boundary have been found at many sites all over the world (Alvarez et al., 1984), and there is considerable evidence that the Ir derives from an earth-impacting extraterrestrial bolide (Alvarez et al. 1980; Izett, 1988).

In addition to Ir we have analyzed the Cretaceous/Tertiary boundary section in Hole 738C for elements such as Fe, Sc, Cr,

Ni, Zn, Co, As, Sb, and rare earth elements (REE). Chemical data for these elements may be relevant for our understanding of how marine Cretaceous/Tertiary boundary clays formed, what composition the Cretaceous/Tertiary boundary extraterrestrial bolide had, and if there were any changes in the elemental composition of seawater associated with the boundary event.

SAMPLES AND ANALYTICAL METHODS

Samples that vertically span distances of 0.2–2 cm were collected from Sections 119-738C-20R-4 and 119-738C-20R-5. Samples were taken continuously every 1 cm from a few centimeters below the base of the laminated Cretaceous/Tertiary boundary clay-rich zone to the top of this zone. Fine laminations extend over the interval from 83.0 to 98.0 cm in Section 119-738C-20R-5. The interval at 96.0–97.0 cm was separated into two parts, an upper layer about 2 mm thick with somewhat darker greenish gray color than the rest of the boundary clay-rich zone and a basal layer about 8 mm thick, with a relatively light color. In addition to the closely spaced samples across the 15-cm-thick laminated zone, samples were collected at about 5- to 20-cm intervals up to a level about 1 m above the top of the laminated interval. During drilling a chert horizon was encountered a few centimeters below the base of the Cretaceous/Tertiary boundary clay-rich zone, and recovery of sediments below the boundary had been seriously disturbed. The exact stratigraphic position of the chalk pieces that were recovered below the chert (Section 119-738C-21-R-1) cannot be determined with certainty; therefore, no samples from this interval were analyzed.

All samples studied were collected by Brian Huber. During sampling any contact of the samples with metal was avoided. The samples were wrapped in plastic film and sent to the Lawrence Berkeley Laboratory for chemical analyses.

At the Lawrence Berkeley Laboratory preparation of the samples and chemical analyses followed the same routine as for the samples from ODP Leg 113 Holes 689B and 690C (see Michel et al., 1990). Iridium analyses were performed with the

¹ Barron, J., Larsen, B., et al., 1991. *Proc. ODP, Sci. Results*, 119: College Station, TX (Ocean Drilling Program).

² Department of Marine Geology, University of Gothenburg, S-402 32 Gothenburg, Sweden.

³ Lawrence Berkeley Laboratory, Berkeley, CA 94720, U.S.A.

⁴ Geological Institute, ETH-Zentrum, CH-8092 Zürich, Switzerland.

⁵ Department of Paleobiology, National Museum of Natural History, Smithsonian Institution, Washington, DC 20560, U.S.A.

Iridium Coincidence Spectrometer (ICS) built at the laboratory for performing rapid, high-resolution analyses of iridium in different geological materials (Michel et al., 1990). The ICS technique takes advantage of the fact that neutron-irradiated Ir emits gamma rays of two different energies (316.5 and 468.1 keV). By discriminating the coincident emission of these gamma rays from background radiation, a very high resolution in the Ir analyses can be obtained. Iridium concentrations were calibrated against the standard "DINO-1" (Alvarez et al., 1982). Analyses of elements other than Ir were performed by conventional INAA (Perlman and Asaro, 1969). Concentration calibrations for these elements (except Zn) were made against "Standard Pottery" (Perlman and Asaro, 1971; revisions have been made for Cr, Alvarez et al., 1982; and Lu and Yb, H. R. Bowman, F. Asaro, and H. V. Michel, unpubl. data).

The errors presented for our analytical data (except for Ir) are estimates of the precision of measurement. The precisions are 1σ values, that is, they represent the standard deviation of the errors in repeated counts of gamma rays. The accuracy of the analyses (except for Ir and Zn) is also influenced by the uncertainties in the abundances of respective element in Standard Pottery (Perlman and Asaro, 1971). These uncertainties are generally less than 1% relative error. For Zn there may be a 10% relative error in the accuracy of the analyses, because it was calibrated vs. a flux monitor (^{45}Sc). The errors presented for Ir are estimates of the accuracy of the analyses.

The Hole 738C samples weighed 100 mg and were irradiated for 10 hr in a neutron flux of 2.5×10^{13} neutrons/s/cm².

PROCESSING OF DATA

All chemical analyses were performed on bulk samples, and the chemical data presented in Tables 1 and 2 represent the results obtained from these analyses.

Because biogenic minerals such as calcite or opaline silica commonly constitute the dominant component in ODP samples, variations in elemental abundances between such samples are mainly governed by variations in the distribution of biogenic debris. (Authigenic components such as pyrite and goethite may sometimes have a similar diluting effect.) A way of disentangling significant variations in the chemistry of the clay fraction of a sediment (without removing the biogenic and authigenic fractions by, for example, acid leaching) is to normalize data for the whole-rock concentrations of the elements of interest vs. the whole-rock concentration of an element that occurs only in the aluminosilicate fraction of the sediment. Through such a normalizing procedure, the diluting effect of calcite, as well as opaline silica, and many authigenic components can be removed. Two elements that generally are considered to be primarily associated with the clay fraction of a sediment are Al and Sc. They occur in very low concentrations in most biogenic minerals and show negligible concentrations in the majority of authigenic minerals that may occur in abundance in marine sediments. Alumina may be authigenically bound to, for example, glauconite or zeolites, however, in these cases the Al may derive from a lithic precursor. Under some circumstances Sc may form authigenic complexes with phosphates, and, in sediments with high concentrations of, for example, skeletal fish debris, a fraction of the Sc may be authigenic (Oudin and Cocherie, 1988); however, in most cases the effect is marginal. Generally speaking, it is preferable to use Al rather than Sc as the "clay indicator." Because we could not measure Al abundances, however, we have used Sc instead.

In presenting element distributions across the Cretaceous/Tertiary boundary in Hole 738C in Figures 1-3, we used the following data processing technique:

$$Y^* = Y/\text{Sc} \times 10 \text{ ppm},$$

where Y is the bulk-sample concentration of the element of interest and Y* is the processed value for the element. The value Y* represents the concentration of Y in the sample if the Sc concentration of the sample was 10 ppm. The value 10 ppm was chosen because this is the Sc content of the most Sc-rich sample in the profile studied. Sc (10 ppm)-normalized data are easier to conceive than simple element/Sc ratios, and comparisons of elemental data between different geological materials is facilitated. The Sc content of average shale is about 15 ppm (Krauskopf, 1979; Taylor and McLennan, 1988).

ELEMENT STRATIGRAPHY ACROSS THE CRETACEOUS/TERTIARY BOUNDARY

Iridium

The distribution of Ir (on a whole-rock basis) across the Cretaceous/Tertiary boundary in Hole 738C is presented in Table 1 and Figures 1 and 2. The Ir values reach a profound peak concentration of 18 ppb in the dark lamina at 96.0-96.2 cm in Section 119-738C-20R-5. Upward from this level, Ir concentrations decrease gradually. Fourteen centimeters above the dark layer, bulk-sample Ir concentrations are still as high as 4 ppb. In the youngest sample that we analyzed, about 115 cm above the Ir-rich dark lamina, Ir concentrations have still not reached background levels. The Ir concentration in this sample is 0.1 ppb, a value that is higher than values typically measured in equivalent calcite-rich ODP samples from stratigraphic levels other than the Cretaceous/Tertiary boundary. For example, calcite-rich background samples from Hole 690C (Michel et al., 1990) yield Ir values of about 0.004-0.02 ppb. The gradual decrease of Ir up-section across the boundary indicates a single input of Ir (detritus-bound, atomized, or dissolved) to the ocean, with subsequent reworking, precipitation from seawater, and settling on the seafloor. The gradual tailing off of the Ir also indicates that the sediments across the boundary represent a relatively continuous and complete section.

Across the interval from the base of the dark lamina at the 96.0-96.2 cm level and downward 5 cm, Ir concentrations are also very high. In the lowermost sample analyzed, from just above the chert that disturbed sediment recovery, Ir concentrations are as high as 1.65 ppb, a value that is two to three orders of magnitude higher than Ir concentrations in typical calcite-rich (non-Cretaceous/Tertiary boundary) ODP samples (Michel et al., 1990).

The integrated amount of Ir across the Cretaceous/Tertiary boundary in Hole 738C is 320 ng Ir/cm². This is one of the highest integrated Ir values measured across a Cretaceous/Tertiary boundary horizon. (When calculating the integrated value we considered the whole interval between the uppermost and lowermost samples studied. A sediment density of 2 g/cm³ was assumed).

What is noteworthy regarding the Ir distribution in Hole 738C is that fine laminations (see Fig. 1) and increased clay content (see subsequent sections about Sc and Fe) start occurring 2-4 cm below the Ir peak at 96.0-96.2 cm.

For comparison the distribution of Sc (10 ppm)-normalized Ir (Ir*) is illustrated in Figure 2. On the whole the Sc-normalized Ir distribution is similar to the whole-rock Ir distribution; however, one important difference exists. Compared to Ir, Ir* shows a much less pronounced peak in the dark lamina at 96.0-96.2 cm. High concentrations of Ir* (13-18 ppb) are instead distributed over an interval of about 5 cm (92-97 cm). This shows that the pronounced sharp peak in whole-rock Ir concentration at 96.0-96.2 cm is an effect partly governed by variations in calcite content. Another interesting fact illustrated in Figure 2 is that the ratios of Ir* to Ir (whole-rock) concentrations are a factor of three to four higher in the 5-cm-thick section below the 96.0-96.2 cm interval than in that interval itself.

Table 1. Instrumental neutron activation analysis results for elements other than the rare earths.

Sample interval in cm	Fe (%)	Sc (ppm)	Ir ^a (ppb)	Cr (ppm)	Co (ppm)	Zn (ppm)	Hf (ppm)	Ta (ppm)	Cs (ppm)	As (ppm)	Sb (ppm)	U (ppm)	Th (ppm)	Ba (ppm)
119 - 738C - 20R - 4														
129 - 130	0.40 ± 0.01	4.89 ± 0.05	0.10 ± 0.01	3.38 ± 0.29	1.41 ± 0.06	32.2 ± 1.7	0.41 ± 0.04	0.059 ± 0.004	0.24 ± 0.01	< 15	< 0.4	0.25 ± 0.05	1.56 ± 0.04	1851 ± 45
119 - 738C - 20R - 5														
3 - 4	0.54 ± 0.01	6.87 ± 0.07	0.18 ± 0.01	4.06 ± 0.34	2.02 ± 0.07	39.2 ± 1.9	0.46 ± 0.05	0.071 ± 0.004	0.24 ± 0.01	< 15	< 0.4	0.25 ± 0.05	1.89 ± 0.04	2707 ± 64
16 - 17	0.67 ± 0.01	7.59 ± 0.08	0.22 ± 0.02	4.52 ± 0.35	2.42 ± 0.07	73.0 ± 2.2	0.50 ± 0.05	0.082 ± 0.004	0.24 ± 0.01	< 15	< 0.4	0.29 ± 0.05	1.98 ± 0.04	2600 ± 61
26 - 27	0.63 ± 0.01	7.25 ± 0.07	0.26 ± 0.01	5.30 ± 0.35	2.16 ± 0.07	48.0 ± 2.0	0.47 ± 0.05	0.072 ± 0.004	0.24 ± 0.01	< 15	< 0.4	0.29 ± 0.05	1.99 ± 0.04	2822 ± 66
33 - 34	0.69 ± 0.01	7.20 ± 0.07	0.29 ± 0.02	6.24 ± 0.35	2.15 ± 0.07	40.7 ± 2.0	0.48 ± 0.05	0.084 ± 0.004	0.26 ± 0.01	< 15	< 0.4	0.33 ± 0.05	2.13 ± 0.04	2785 ± 65
43 - 44	0.76 ± 0.01	7.63 ± 0.08	0.39 ± 0.02	6.73 ± 0.37	2.51 ± 0.08	91.1 ± 2.4	0.66 ± 0.05	0.093 ± 0.004	0.29 ± 0.01	< 15	< 0.4	0.34 ± 0.06	2.36 ± 0.05	2799 ± 90
55 - 56	0.90 ± 0.01	8.40 ± 0.08	0.52 ± 0.04	8.58 ± 0.40	3.15 ± 0.09	53.7 ± 2.2	0.83 ± 0.06	0.098 ± 0.004	0.34 ± 0.01	< 15	< 0.4	0.29 ± 0.06	2.80 ± 0.05	3027 ± 97
66 - 67	1.01 ± 0.01	9.01 ± 0.09	0.92 ± 0.06	12.15 ± 0.42	4.22 ± 0.10	74.6 ± 2.5	0.73 ± 0.06	0.107 ± 0.005	0.36 ± 0.01	< 15	< 0.4	0.26 ± 0.06	2.92 ± 0.05	3698 ± 117
76 - 78	0.73 ± 0.01	7.72 ± 0.08	1.28 ± 0.07	9.15 ± 0.38	3.07 ± 0.08	47.7 ± 2.1	0.51 ± 0.05	0.086 ± 0.004	0.34 ± 0.01	< 15	< 0.4	0.46 ± 0.06	2.30 ± 0.05	3211 ± 102
82 - 83	1.17 ± 0.01	8.91 ± 0.09	4.24 ± 0.29	32.10 ± 0.53	4.37 ± 0.10	60.5 ± 2.4	0.86 ± 0.06	0.134 ± 0.005	0.55 ± 0.01	< 15	< 0.4	0.51 ± 0.07	2.89 ± 0.05	4272 ± 135
83 - 84	1.28 ± 0.01	9.17 ± 0.09	5.54 ± 0.26	48.17 ± 0.62	4.90 ± 0.11	56.6 ± 2.5	0.93 ± 0.06	0.149 ± 0.005	0.68 ± 0.01	< 15	< 0.4	0.64 ± 0.07	3.25 ± 0.05	4417 ± 139
84 - 85	1.24 ± 0.01	9.09 ± 0.09	5.10 ± 0.25	36.53 ± 0.54	4.79 ± 0.10	61.3 ± 2.5	0.75 ± 0.06	0.137 ± 0.005	0.62 ± 0.02	< 15	< 0.4	0.56 ± 0.07	3.13 ± 0.05	4398 ± 101
85 - 86	1.23 ± 0.01	8.66 ± 0.09	6.02 ± 0.34	35.14 ± 0.52	4.57 ± 0.10	58.6 ± 2.4	0.86 ± 0.06	0.127 ± 0.005	0.60 ± 0.01	< 15	0.32 ± 0.10	0.45 ± 0.06	2.91 ± 0.05	4534 ± 104
86 - 87	1.46 ± 0.01	8.82 ± 0.09	5.50 ± 0.37	46.11 ± 0.57	5.08 ± 0.10	67.0 ± 2.5	0.86 ± 0.06	0.143 ± 0.005	0.73 ± 0.02	< 15	< 0.4	0.61 ± 0.07	3.25 ± 0.05	4666 ± 107
87 - 88	1.13 ± 0.01	8.24 ± 0.08	6.05 ± 0.33	33.99 ± 0.51	4.44 ± 0.10	51.5 ± 2.3	0.79 ± 0.06	0.118 ± 0.005	0.52 ± 0.01	< 15	0.32 ± 0.10	0.53 ± 0.06	2.69 ± 0.05	3959 ± 92
88 - 89	1.01 ± 0.01	7.42 ± 0.07	5.95 ± 0.40	34.83 ± 0.50	3.56 ± 0.09	50.3 ± 2.2	0.61 ± 0.05	0.102 ± 0.005	0.47 ± 0.01	< 15	< 0.4	0.41 ± 0.06	2.45 ± 0.05	3640 ± 85
89 - 90	1.09 ± 0.01	7.67 ± 0.08	6.17 ± 0.40	37.79 ± 0.52	4.05 ± 0.09	50.2 ± 2.3	0.71 ± 0.06	0.113 ± 0.005	0.49 ± 0.01	< 15	< 0.4	0.46 ± 0.05	2.47 ± 0.05	3581 ± 83
90 - 91	1.02 ± 0.01	6.60 ± 0.07	7.53 ± 0.48	37.87 ± 0.51	3.29 ± 0.08	46.8 ± 2.1	0.62 ± 0.05	0.094 ± 0.004	0.44 ± 0.00	< 15	< 0.4	0.45 ± 0.05	2.29 ± 0.05	3475 ± 81
91 - 92	1.20 ± 0.01	6.86 ± 0.07	8.05 ± 0.48	46.97 ± 0.55	4.01 ± 0.09	50.0 ± 2.2	0.61 ± 0.05	0.101 ± 0.004	0.46 ± 0.01	< 15	< 0.4	0.46 ± 0.05	2.34 ± 0.05	3448 ± 80
92 - 93	1.20 ± 0.01	7.00 ± 0.07	9.33 ± 0.51	51.96 ± 0.63	4.45 ± 0.10	63.1 ± 2.3	0.68 ± 0.06	0.101 ± 0.005	0.45 ± 0.00	< 15	< 0.4	0.43 ± 0.05	2.38 ± 0.05	3462 ± 111
93 - 94	1.26 ± 0.01	7.04 ± 0.07	9.67 ± 0.52	56.39 ± 0.60	4.87 ± 0.10	51.6 ± 2.3	0.57 ± 0.05	0.098 ± 0.005	0.48 ± 0.01	< 15	< 0.4	0.49 ± 0.05	2.45 ± 0.05	3468 ± 81
94 - 95	1.42 ± 0.01	7.49 ± 0.07	10.45 ± 0.48	64.70 ± 0.64	5.73 ± 0.11	62.5 ± 2.4	0.76 ± 0.06	0.105 ± 0.005	0.53 ± 0.01	< 15	< 0.4	0.45 ± 0.05	2.51 ± 0.05	3694 ± 86
95 - 96	1.90 ± 0.02	9.49 ± 0.09	13.54 ± 0.76	126.40 ± 1.26	9.75 ± 0.15	107.4 ± 2.3	0.93 ± 0.06	0.140 ± 0.005	0.60 ± 0.01	< 15	0.42 ± 0.11	0.57 ± 0.05	3.28 ± 0.05	3968 ± 92
96.0 - 96.2	2.21 ± 0.02	10.28 ± 0.10	17.76 ± 0.50	214.50 ± 2.14	12.66 ± 0.17	555.0 ± 6.0	0.95 ± 0.06	0.122 ± 0.005	0.61 ± 0.02	< 15	0.75 ± 0.13	0.42 ± 0.05	3.25 ± 0.06	2919 ± 69
96.2 - 97.0	0.61 ± 0.01	4.86 ± 0.05	7.71 ± 0.57	59.67 ± 0.58	4.86 ± 0.10	211.6 ± 3.1	0.33 ± 0.05	0.067 ± 0.004	0.29 ± 0.01	< 15	0.43 ± 0.09	0.51 ± 0.05	1.89 ± 0.04	2416 ± 59
97 - 98	0.38 ± 0.01	3.34 ± 0.03	2.54 ± 0.09	13.34 ± 0.33	2.71 ± 0.07	43.1 ± 1.8	0.17 ± 0.04	0.035 ± 0.003	0.15 ± 0.01	< 15	< 0.4	0.61 ± 0.04	0.76 ± 0.03	1306 ± 45
98 - 99	0.24 ± 0.01	2.69 ± 0.03	2.13 ± 0.09	8.12 ± 0.27	1.02 ± 0.05	25.3 ± 1.4	0.18 ± 0.03	0.031 ± 0.003	0.11 ± 0.01	< 15	< 0.4	0.59 ± 0.04	0.58 ± 0.03	912 ± 33
99 - 100	0.21 ± 0.01	2.48 ± 0.02	1.79 ± 0.10	6.13 ± 0.25	0.79 ± 0.04	19.2 ± 1.3	0.14 ± 0.03	0.023 ± 0.003	0.09 ± 0.01	< 15	< 0.4	0.70 ± 0.04	0.52 ± 0.03	791 ± 30
100 - 101	0.18 ± 0.01	2.28 ± 0.02	1.64 ± 0.09	5.69 ± 0.24	0.71 ± 0.04	18.7 ± 1.3	0.10 ± 0.03	0.025 ± 0.003	0.08 ± 0.01	< 15	< 0.4	0.60 ± 0.04	0.41 ± 0.03	743 ± 28
101 - 102	0.19 ± 0.01	2.25 ± 0.02	1.65 ± 0.09	5.03 ± 0.24	0.71 ± 0.04	17.8 ± 1.3	0.10 ± 0.03	0.029 ± 0.003	0.09 ± 0.01	< 15	< 0.4	0.74 ± 0.04	0.51 ± 0.03	792 ± 30

a

Iridium Coincidence Spectrometer results.

Table 2. Instrumental neutron activation analysis results for rare earth elements.

Sample interval in cm	La (ppm)	Ce (ppm)	Sm (ppm)	Eu (ppm)	Tb (ppm)	Yb (ppm)	Lu (ppm)
119 - 738C - 20R - 4							
129 - 130	22.8 ± 0.6	14.8 ± 0.6	3.95 ± 0.02	0.94 ± 0.01	0.62 ± 0.03	1.91 ± 0.05	0.29 ± 0.01
119 - 738C - 20R - 5							
3 - 4	26.0 ± 0.7	19.7 ± 0.7	4.92 ± 0.02	1.16 ± 0.01	0.75 ± 0.03	2.35 ± 0.06	0.33 ± 0.01
16 - 17	29.4 ± 0.7	21.2 ± 0.7	5.13 ± 0.02	1.23 ± 0.01	0.84 ± 0.04	2.60 ± 0.06	0.37 ± 0.02
26 - 27	26.9 ± 0.7	20.3 ± 0.7	4.79 ± 0.02	1.16 ± 0.01	0.77 ± 0.03	2.60 ± 0.06	0.36 ± 0.02
33 - 34	28.0 ± 0.7	23.1 ± 0.8	5.02 ± 0.02	1.21 ± 0.01	0.82 ± 0.03	2.72 ± 0.06	0.37 ± 0.02
43 - 44	28.2 ± 0.8	22.8 ± 0.8	5.24 ± 0.02	1.24 ± 0.01	0.82 ± 0.05	2.69 ± 0.08	0.39 ± 0.02
55 - 56	32.1 ± 0.8	25.3 ± 0.9	5.32 ± 0.02	1.31 ± 0.01	0.86 ± 0.05	2.71 ± 0.08	0.39 ± 0.02
66 - 67	29.9 ± 0.8	26.7 ± 0.9	5.79 ± 0.03	1.40 ± 0.02	0.94 ± 0.05	2.93 ± 0.08	0.37 ± 0.02
76 - 78	27.9 ± 0.7	22.0 ± 0.8	5.21 ± 0.02	1.17 ± 0.01	0.81 ± 0.04	2.53 ± 0.07	0.38 ± 0.02
82 - 83	42.9 ± 0.9	39.4 ± 1.0	7.92 ± 0.03	1.91 ± 0.02	1.37 ± 0.07	3.93 ± 0.10	0.51 ± 0.02
83 - 84	52.0 ± 1.0	44.0 ± 1.1	9.29 ± 0.03	2.10 ± 0.02	1.49 ± 0.07	3.91 ± 0.10	0.55 ± 0.02
84 - 85	46.2 ± 0.9	43.5 ± 1.0	8.96 ± 0.03	2.19 ± 0.02	1.52 ± 0.05	4.17 ± 0.09	0.56 ± 0.02
85 - 86	41.6 ± 0.9	37.1 ± 1.0	7.78 ± 0.03	1.80 ± 0.02	1.27 ± 0.05	3.68 ± 0.08	0.50 ± 0.02
86 - 87	50.6 ± 1.0	40.7 ± 1.0	10.00 ± 0.03	2.10 ± 0.02	1.44 ± 0.06	3.82 ± 0.09	0.55 ± 0.02
87 - 88	43.0 ± 0.9	35.5 ± 0.9	7.94 ± 0.03	1.79 ± 0.02	1.33 ± 0.05	3.63 ± 0.08	0.50 ± 0.02
88 - 89	36.0 ± 0.8	31.2 ± 0.8	6.82 ± 0.03	1.53 ± 0.01	1.07 ± 0.04	3.24 ± 0.08	0.44 ± 0.02
89 - 90	37.9 ± 0.7	30.7 ± 0.9	7.06 ± 0.02	1.67 ± 0.01	1.17 ± 0.05	3.44 ± 0.08	0.45 ± 0.02
90 - 91	36.5 ± 0.6	27.7 ± 0.8	6.58 ± 0.02	1.43 ± 0.01	1.00 ± 0.04	3.05 ± 0.07	0.39 ± 0.02
91 - 92	36.1 ± 0.6	26.3 ± 0.8	6.64 ± 0.02	1.44 ± 0.01	1.08 ± 0.04	2.85 ± 0.07	0.40 ± 0.02
92 - 93	37.4 ± 0.7	29.7 ± 0.9	7.09 ± 0.03	1.53 ± 0.02	1.13 ± 0.06	3.19 ± 0.09	0.48 ± 0.02
93 - 94	38.3 ± 0.7	28.3 ± 0.9	7.30 ± 0.02	1.60 ± 0.01	1.21 ± 0.05	3.04 ± 0.07	0.43 ± 0.02
94 - 95	38.2 ± 0.7	28.5 ± 0.9	7.42 ± 0.02	1.67 ± 0.01	1.24 ± 0.05	2.98 ± 0.07	0.42 ± 0.02
95 - 96	40.1 ± 0.7	28.6 ± 0.9	8.46 ± 0.03	1.84 ± 0.02	1.25 ± 0.05	2.79 ± 0.07	0.40 ± 0.02
96.0 - 96.2	34.4 ± 0.7	22.9 ± 0.9	7.90 ± 0.02	1.69 ± 0.01	1.25 ± 0.05	2.30 ± 0.07	0.32 ± 0.02
96.2 - 97.0	41.3 ± 0.7	27.3 ± 0.8	8.35 ± 0.03	1.84 ± 0.02	1.34 ± 0.05	3.03 ± 0.07	0.43 ± 0.02
97 - 98	28.3 ± 0.6	15.3 ± 0.6	4.57 ± 0.02	0.97 ± 0.01	0.72 ± 0.04	2.24 ± 0.07	0.33 ± 0.02
98 - 99	23.6 ± 0.5	12.6 ± 0.5	3.51 ± 0.02	0.75 ± 0.01	0.57 ± 0.03	2.06 ± 0.06	0.32 ± 0.02
99 - 100	22.0 ± 0.5	11.8 ± 0.5	3.14 ± 0.02	0.69 ± 0.01	0.57 ± 0.03	1.97 ± 0.06	0.30 ± 0.02
100 - 100	21.5 ± 0.5	11.5 ± 0.5	2.96 ± 0.02	0.64 ± 0.01	0.50 ± 0.03	1.87 ± 0.06	0.30 ± 0.02
101 - 102	21.3 ± 0.5	10.9 ± 0.5	2.99 ± 0.02	0.64 ± 0.01	0.53 ± 0.03	1.96 ± 0.06	0.33 ± 0.02

The third graph in Figure 2 illustrates the Fe (2.2%)-normalized Ir distribution across the K/T boundary (the value 2.2% Fe was chosen as normalizing standard because the Fe content on a whole-rock basis of the most clay-rich sample in the interval studied is 2.2%). The major Ir/Fe x 2.2% peak occurs in the interval below the dark clay at 96.0–96.2 cm. One explanation for this may be that Ir but not Fe has diffused downsection from the clay at 96.0–96.2 cm. An alternative interpretation is that an authigenic iron-rich component (possibly a glauconitic clay mineral) is heterogeneously distributed throughout the clay-rich interval, but is absent in the clay-poor sections below 96.0–96.2 cm. This interpretation could also explain the irregular appearance of Ir/Fe ratios across the laminated clay-rich interval (see also the following discussion about Fe distribution).

Scandium

High concentrations of Sc occur throughout the whole 15-cm-thick laminated Cretaceous/Tertiary boundary interval (Fig. 3). Scandium concentrations are roughly proportional to the amount of clay present in the sediment; accordingly the Sc distribution shows a negative correlation with the calcite distribution displayed in Figure 1. Highest Sc concentrations are measured in the dark lamina at 96.0–96.2, and in the 95.0–96.0 cm interval just above this level. The lowest calcite content (69%) of the section has been measured in these two layers. A notable fact is that in the upper part of the laminated interval (83–87 cm) Sc concentrations (up to 9.2 ppm) are almost as high as in the 96.0–96.2 cm interval (10.3 ppm Sc). This is consistent with

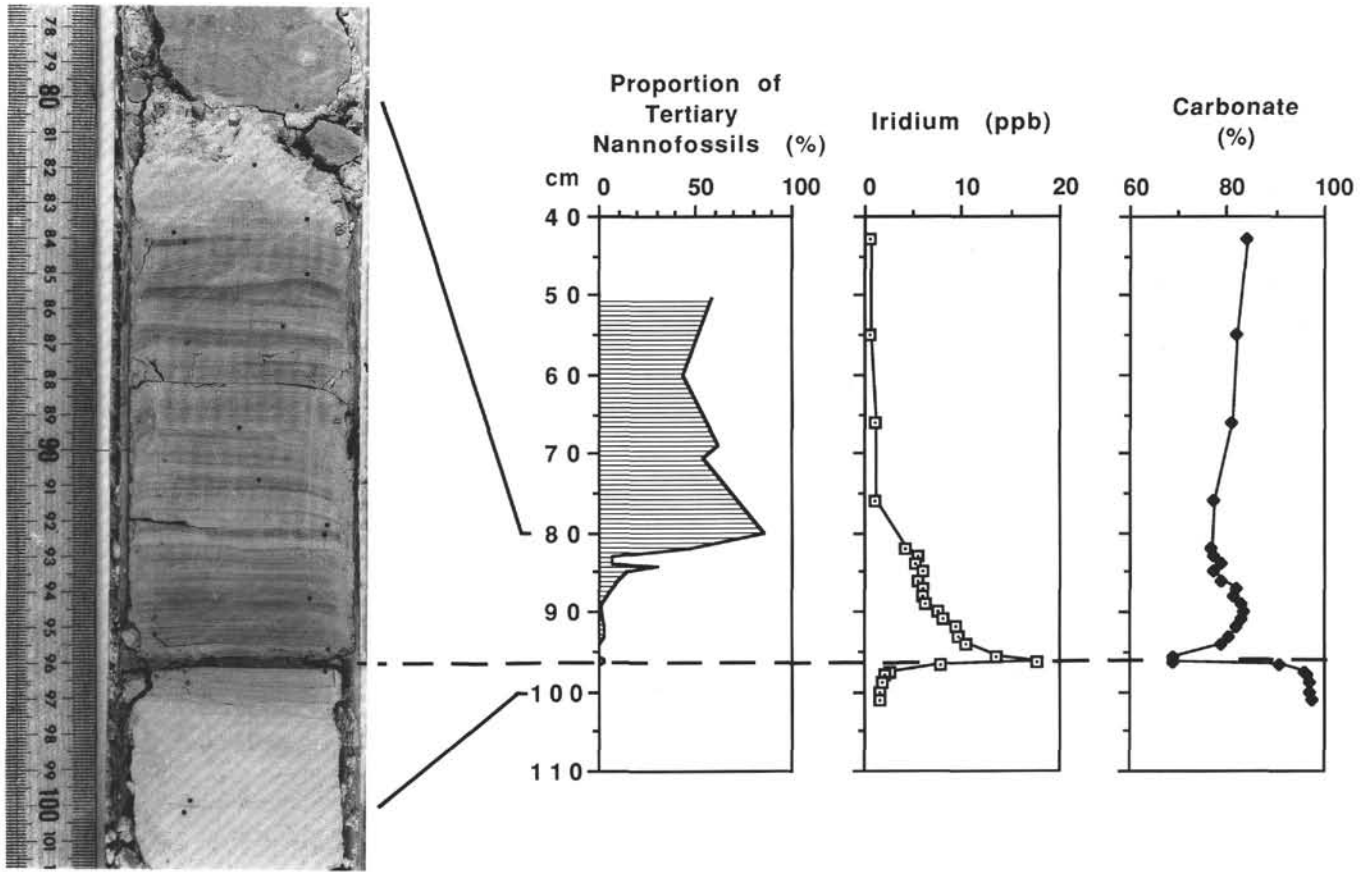


Figure 1. The Cretaceous/Tertiary boundary interval in ODP Hole 738C. Notice that fine laminations begin a few centimeters below the Ir peak. The first Tertiary foraminifers appear in the laminated interval below the Ir peak (Huber, this volume). Carbonate data are discussed in Thierstein et al. (this volume).

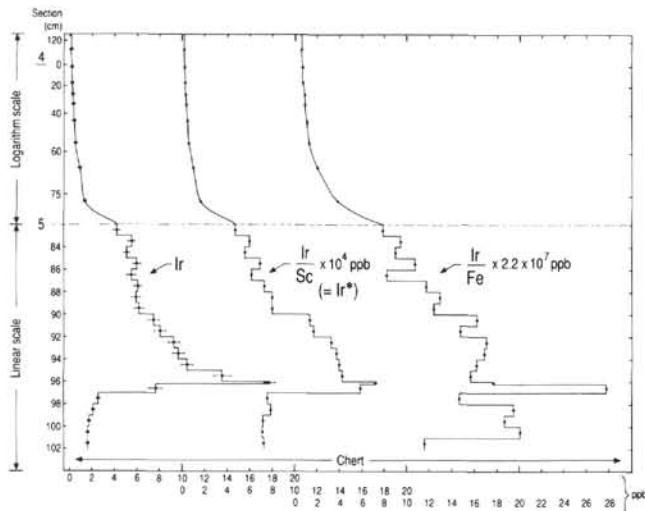


Figure 2. The distribution of Ir (whole-rock), Sc (10 ppm)-normalized Ir, and Fe (2.2%)-normalized Ir across the Cretaceous/Tertiary boundary in Sections 119-738C-20R-4 and 119-738C-20R-5.

the circumstance that calcite content is only a factor of 1.1 higher (77% calcite) in the upper laminated interval than in the 96.0–96.2 cm interval.

An important fact illustrated in Figure 3 is that enhanced Sc concentrations compared to background extend for additionally

at least 80 cm above the laminated interval. This means that the Cretaceous/Tertiary boundary in Hole 738C is characterized by a zone of about 1 m of sediments with substantially higher clay content than the sediments above and below this interval. Examination of photos of the core sections from which our samples were collected confirms that the Sc-rich interval, about 1 m thick, across the Cretaceous/Tertiary boundary has a significantly darker color than the very white chalks below and above this interval. The basal 15 cm of the clay-rich interval is finely laminated. The laminations begin about 2 cm below the Ir peak at 96.0–96.2 cm (see Fig. 1); however, Sc concentrations show a gradual increase upward beginning about 4 cm below the maximum Ir peak.

Iron

Iron can be used to distinguish variations in the amounts of biogenic vs. nonbiogenic components in a sediment. Iron, however, shows a broad spectrum of authigenic mineral phases in which it may occur, and interpretations of its distribution pattern are therefore enigmatic. Most of the Fe in deep-sea sediments occurs in clay minerals and other siliciclastic detritus.

The Fe distribution in Hole 738C confirms the overall trend observed in the distribution of Sc (Fig. 3). Increased Fe concentrations occur over an interval of about 1 m, the same interval with a dark coloring and increased Sc concentrations. If all iron was bound in the same mineral phase as Sc, the Sc (10 ppm)-normalized distribution of Fe (i.e., Fe*) would show a straight line across the Cretaceous/Tertiary boundary. Indeed, the Fe* distribution is more flattened than the Fe (whole-rock) distribution; however, a significant excess of Fe (compared with Sc) oc-

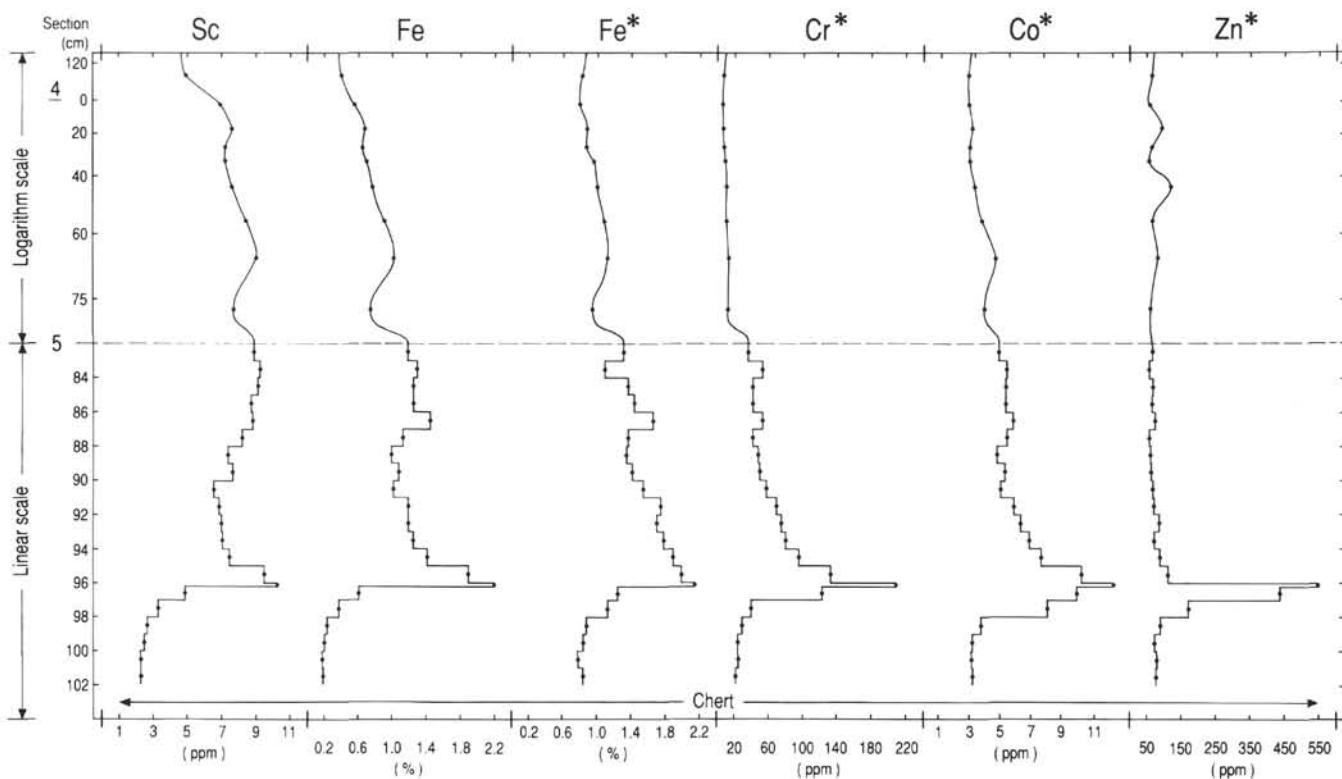


Figure 3. The distribution of Sc and Fe (whole-rock), and Sc (10 ppm)-normalized abundances of Fe, Cr, Co, and Zn across the Cretaceous/Tertiary boundary in Sections 119-738C-20R-4 and 119-738C-20R-5.

curs throughout much of the laminated interval (Fig. 3). This Fe most likely occurs in another phase than the Sc. Excess iron shows a peak in the 96.0–96.2 cm interval and decreases somewhat upward, which could indicate that the iron derives from, for example, an iron-rich extraterrestrial phase. However, the excess iron content is almost as high in, for example, the interval from 86 to 87 cm as in the 96.0–96.2 cm interval. The upper iron-rich layer has Ir* concentrations lower by a factor of three than the lower iron-rich layer. Excess Fe/excess Ir ratios would be similar between the two levels if both elements occur in the same phase. Because the ratios increase upward across the laminated interval, it is likely that a major fraction of the excess iron is due to an authigenic iron-rich phase that occurs throughout the clay-rich laminated section. This fact together with a greenish gray color of the clay-rich layers could indicate presence of a few percent of some kind of glauconitic mineral and suboxic, slightly reducing conditions during deposition. The unbioturbated nature of the basal clay-rich zone also suggests relatively low Eh conditions during deposition. Thierstein et al. (this volume) did not detect any glauconitic minerals in the laminated interval, however, the green minerals may be present as a thin film primarily on the calcite and could have been lost during carbonate removal prior to the X-ray diffraction analysis.

Chromium

The Sc-normalized Cr distribution shows a consistent trend across the Cretaceous/Tertiary boundary (Fig. 3). The maximum concentration of Cr* occurs in the dark layer at 96.0–96.2 cm, and from there excess Cr compared with Sc decreases gradually up and down along the section. The pronounced Cr anomaly associated with the Ir anomaly in the Hole 738C Cretaceous/Tertiary boundary is interesting insofar that the Cr/Ir ratios are too high to represent iron asteroidal matter. The ratios

lie closer to those reported for chondritic or stony-iron meteorites (see Cr/Ir ratios for meteorites; e.g., in Wedepohl, 1969).

Cobalt

This element also shows an abundance peak near the base of the laminated interval (Table 1 and Sc-normalized data in Fig. 3). Like Ir and Cr, Co is concentrated in extraterrestrial matter, and the excess Co in the Hole 738C Cretaceous/Tertiary sequence most likely ultimately derives from an extraterrestrial bolide. The Co concentration in Hole 738C (13 ppm), however, is very small compared with Co concentrations (190–500 ppm) measured in anoxic, very Ir-rich Cretaceous/Tertiary boundary clays in Denmark, Spain, and New Zealand (Schmitz, 1988b). There are no indications in the form of abundant pyrite or organic matter that strongly reducing conditions occurred in the Hole 738C Cretaceous/Tertiary boundary zone. Instead, suboxic conditions may have prevailed during deposition (see earlier section about Fe distribution). Co/Ir and Co/Cr ratios in the basal Cretaceous/Tertiary boundary interval are significantly to somewhat lower than in most types of extraterrestrial matter (see data for meteorites in Wedepohl, 1969), indicating, perhaps, that some Co has diffused out of the boundary region.

Arsenic, Antimony, and Zinc

These elements represent an enigma in Cretaceous/Tertiary boundary geochemistry. The elements have low abundances in meteorites, but are concentrated in many Cretaceous/Tertiary boundary clays (see, e.g., Schmitz, 1988b). Schmitz (1988b) and Schmitz et al. (1988) argued that the elements show highest abundances in anoxic Cretaceous/Tertiary boundary clays and that they have precipitated as sulfides from seawater. In the clay-rich Cretaceous/Tertiary boundary zone of Hole 738C, no significant As or Sb enrichments were found (Table 1). Arsenic

concentrations lie below our detection limit (15 ppm) in all samples studied. Antimony lies just at or slightly above our detection limit (0.4 ppm). The low As and Sb concentrations in the suboxic boundary interval in Hole 738C give additional support for the notion of a relation between strongly anoxic conditions, abundant sulfide occurrence, and high concentrations of these two elements. For comparison, one layer of the anoxic Caravaca Cretaceous-Tertiary boundary clay contains 600 ppm As and 16 ppm Sb (Schmitz, 1988b).

A very enigmatic finding in the Hole 738C core is a profound Zn enrichment (555 ppm) in the interval 96.0–96.2 cm (Table 1 and Fig. 3). The phase-partitioning of Zn in the layer must be known before any meaningful interpretation of this abundance anomaly can be made. Absorption onto extraterrestrial material or existence of a Zn-rich authigenic phase are two possible explanations for the Zn anomaly.

Barium

Whole-rock Ba concentrations increase from less than 1000 ppm below the Cretaceous/Tertiary boundary to 3000–4700 ppm in the clay-rich boundary interval (Fig. 4). In deep-sea sediments, the bulk of the barium is associated with authigenic or biogenic barite (Goldberg and Arrhenius, 1958; Boström et al. 1973, 1979; Church, 1979; Dehairs et al., 1980). It is known that Ba (and barite) concentrations are high in sediments below biological high-productivity zones (see Schmitz, 1987, and references therein), however, the causal relation between organic productivity in the ocean surface waters and barite production is not well understood (Schmitz, 1987). In Hole 738C the higher Ba (whole-rock) concentrations of the laminated Cretaceous/Tertiary boundary interval compared to those of the underlying chalks could be due either to increased organic productivity during deposition of the boundary interval or to decreased cal-

cite sedimentation rates in connection with constant surface-water barite production.

The Sc-normalized Ba distribution (Ba^*) gives further insight about the behavior of Ba (Fig. 4). The Ba^* values are about 3000–3500 ppm below the boundary laminated interval and increase to values around 4000–5000 ppm in the laminated interval (with the exception of the level at 96.0–96.2 cm). Apparently the rate of barite deposition has increased also relative to the rate of deposition of Sc-carrying clay. This makes it likely that the increase in Ba (and Ba^*) reflects an increase in surface-water productivity, possibly related to the occurrence of nutrient upwelling during deposition of the laminated interval.

Whereas the bulk of the laminated interval shows enhanced Ba and Ba^* concentrations compared to the chalks below, the very Ir-rich layer at 96.0–96.2 cm shows a pronounced negative Ba^* anomaly. This could reflect that the rate of deposition of this layer was high and surface productivity was constant, or that surface organic productivity was suppressed, whereas the rate of clay deposition was constant. Our data give no definite clue as to what may have happened. In many Cretaceous/Tertiary boundary profiles the maximum Ir anomaly coincides with a sharp drop in $\delta^{13}C$ values for the biogenic calcite (e.g., Zachos and Arthur, 1986; Margolis et al., 1987). This negative $\delta^{13}C$ anomaly is commonly thought of as evidence for a decrease in surface-water productivity (e.g., Zachos and Arthur, 1986). It could be that the low Ba^* concentration at 96.0–96.2 cm is a manifestation of this process.

Thorium and Uranium

Neither Th nor U show significantly higher concentrations in extraterrestrial matter than in most types of terrestrial materials. As could be expected, no peaks in the distribution of these elements occur in the strongly Ir-rich layer at 96.0–96.2 cm (Ta-

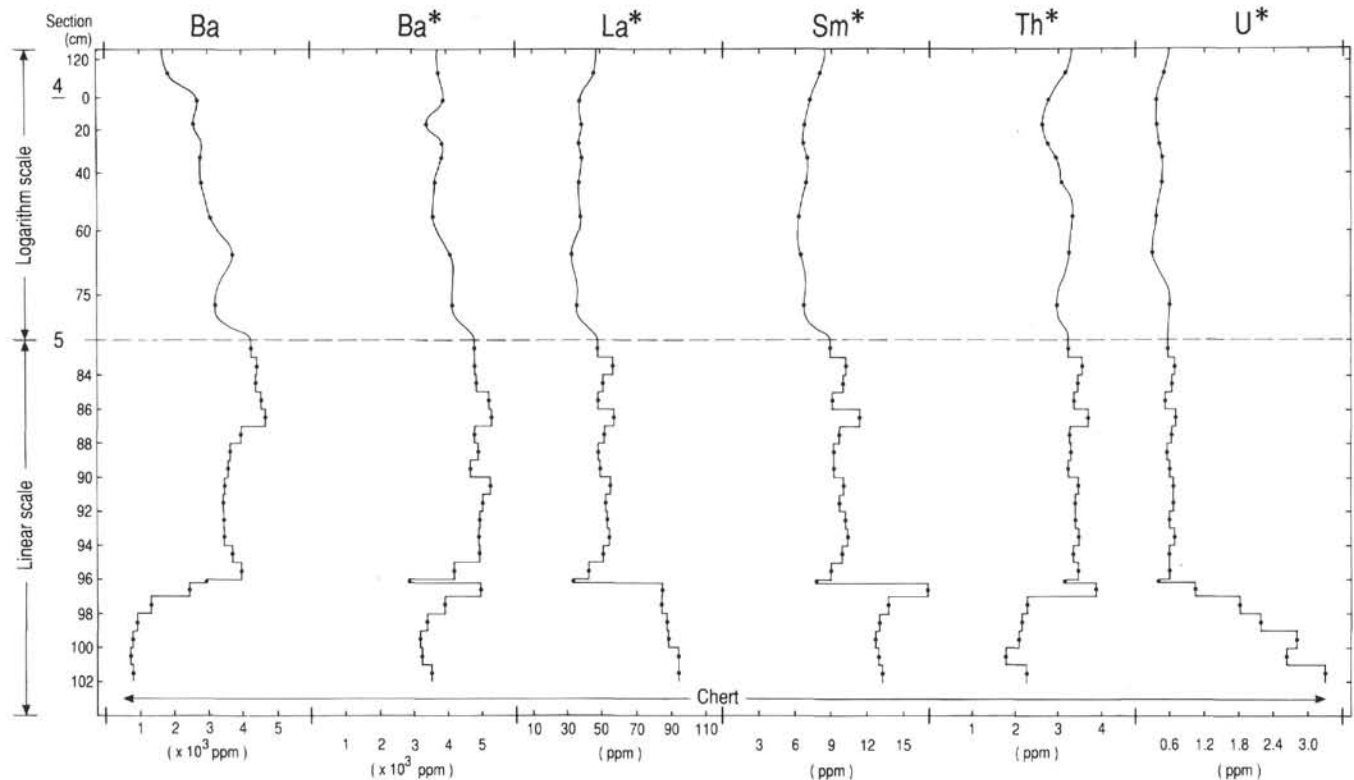


Figure 4. The distribution of Ba (whole-rock) and Sc (10 ppm)-normalized abundances of Ba, La, Sm, Th, and U across the Cretaceous/Tertiary boundary in Sections 119-738C-20R-4 and 119-738C-20R-5.

ble 1 and Fig. 4). Instead the distribution patterns of Th* and U* are almost straight lines across most of the laminated Cretaceous/Tertiary boundary interval. The dark interval at 96.0–96.2 cm shows similar Th* and U* concentrations as all overlying intervals. This could indicate that the bulk of the clay in the dark lamina represents the same kind of material that occurs throughout the overlying sediment section (see the following discussion). The low concentrations of Th* (3.3 ppm) and U* (0.42 ppm) imply that the bulk fraction of these elements has to be detrital rather than authigenic.

In the interval below the lamina at 96.0–96.2 cm both Th* and U* show different concentrations than higher up. This may reflect different provenances of the clay below and above the 96.2 cm level.

Hafnium, Tantalum, and Cesium

The Sc-normalized abundances of these three elements follow the same pattern as Th* and U*. From the base of the 96.0–96.2 cm interval and upward throughout the laminated interval, abundances of Hf*, Ta*, and Cs* show only insignificant variations (see data in Tables 1 and 3). This further supports that the clay from 96.2 cm and upward is made up of the same type of material throughout (see the following discussion).

Below 96.2 cm the concentrations of Hf*, Ta*, and Cs* differ from those measured across the overlying 1-m-thick interval. This is consistent with the trend noticed for Th* and U*.

Rare Earth Elements

Analytical data for these elements are presented in Table 2. Figure 5 displays the REE distribution normalized relative to the REE distribution in average shale (Taylor and McLennan, 1988; see caption for Fig. 5) and the average-shale-normalized La content in respective sample. The most prominent feature of the REE patterns is the negative Ce anomaly, indicating that the bulk of the REE in the samples is derived from seawater and is primarily authigenically bound to biogenic phosphates. From our data it is not possible to determine in detail the amount of seawater-derived vs. clay-associated REE. The process of REE absorption from seawater on biogenic apatite in sediments is discussed in Elderfield and Pagett (1986), Wright et al. (1987), and Oudin and Cocherie (1988), among others.

The average-shale-normalized REE patterns displayed in Figure 5 show a gradual change across the Cretaceous/Tertiary boundary in Hole 738C. The Ce/La ratio is relatively constant across the section studied. However, the remaining REE/La ratios change in a consistent pattern. The ratios of Sm/La, Eu/La, and Tb/La increase markedly from below the laminated interval. They reach maximum values in the 96.0–96.2 cm interval and gradually return to lower values upward in the section. The La-normalized ratios of the heavy REE, Yb, and Lu show the opposite trend. Whether the observed trend reflects an actual change in seawater REE composition in connection with the Cretaceous/Tertiary boundary event or reflects a change in the ratios between seawater-derived and clay-bound REE is difficult to determine from our data. However, if changes attributable to changes in clay REE composition have occurred, a pronounced change in the Ce/La ratio would be expected too. The varying REE patterns across the Cretaceous/Tertiary boundary could also reflect a change in the physicochemical conditions of the diagenetic environment at Hole 738C. Elderfield and Pagett (1986) showed that authigenic REE patterns in sediments are governed not only by the REE composition of seawater, but also by fractionation processes during precipitation of the REE in the sediment. Redox conditions and pH may be factors governing the fractionation processes.

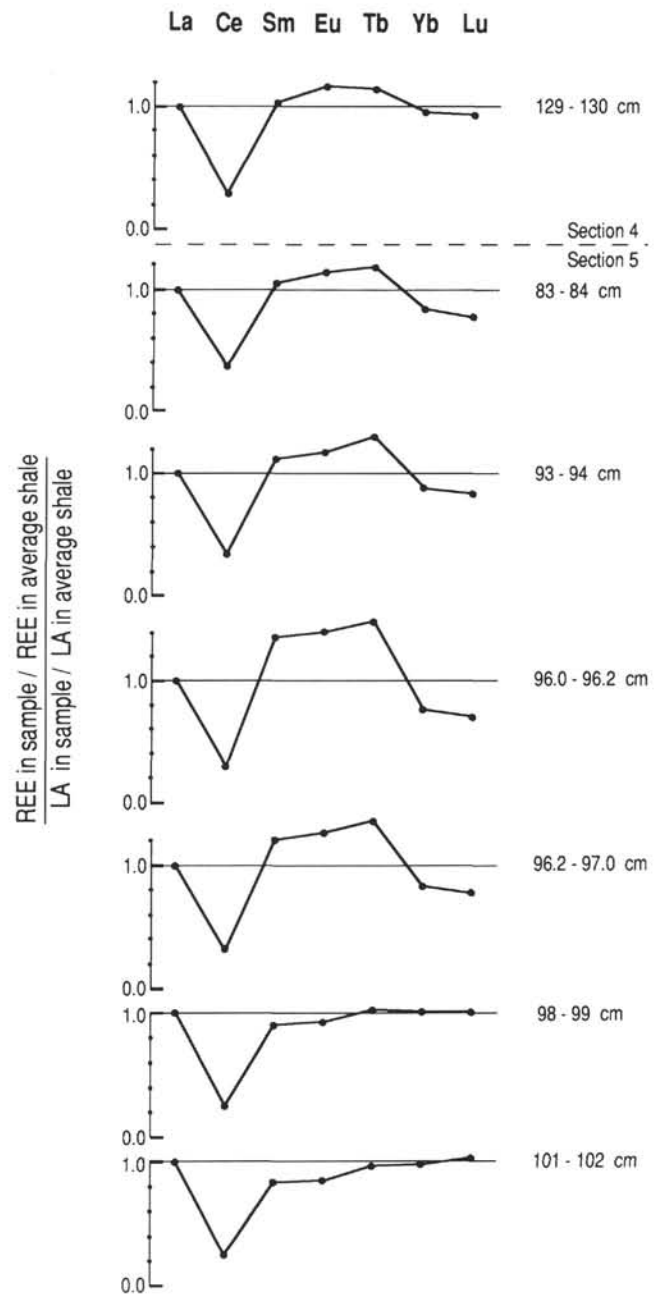


Figure 5. REE abundances normalized vs. average shale and average-shale-normalized La in Sections 119-738C-20R-4 and 119-738C-20R-5. As the average shale standard we used the weighted mean for the REE concentrations in North American Shale Composite (NASC; a composite of 40 North American shale samples), and Post-Archean Average Australian Shale (PAAS, a composite of 23 shale samples from Australia) (Haskin et al., 1968; Table 23 in Taylor and McLennan, 1988).

ORIGIN OF THE IR ANOMALY AND THE CRETACEOUS/TERTIARY BOUNDARY CLAY

At the palynologically defined Cretaceous/Tertiary boundary in nonmarine deposits in the Western Interior of North America (Tschudy and Tschudy, 1986), a distinct, thin (2–3 cm) claystone/clay layer has been found. This layer shows most of

the mineralogical and chemical features that one could expect from an asteroid impact-ejecta fallout layer (Izett, 1988). This includes high Ir concentrations, 35% shocked quartz of total quartz fraction, and the absence of significant amounts of typical volcanic minerals. Considering this, it seems very likely that the global marine Cretaceous/Tertiary boundary Ir anomalies are also linked to the impact of an extraterrestrial bolide on Earth (Alvarez et al., 1980). Schmitz (1988a; 1988b; 1990), however, compared a number of worldwide distributed Ir-rich marine Cretaceous/Tertiary boundary clays with nonmarine boundary clays from the Western Interior and questioned whether the marine boundary clays represent impact-ejecta fallout layers. Schmitz argued that the bulk of the mass of the marine clays is instead made up of locally derived material and that the formation of the clays is due to an oceanic process that in some way is coupled to a bolide impact, possibly on the North American continent.

At Hole 738C the fundamental question to be considered is whether the clay in any part of the Cretaceous/Tertiary boundary section is predominantly made up of altered dust from a world-encompassing impact-ejecta dust cloud. According to the Alvarez et al. (1980) impact scenario, globally distributed Cretaceous/Tertiary boundary clays represent impact-produced dust that settled on the seafloor. The dust was assumed to represent a mixture of predominantly melted impact-target rock and a smaller fraction of pure asteroidal matter (see also Kastner et al., 1984). There are three possibilities to consider for Hole 738C: (1) the clay of the whole 1-m-thick Cretaceous/Tertiary boundary clay-rich zone represents impact-ejecta fallout material, (2) only the clay of the 15-cm-thick laminated interval represents such material, or (3) the clay of the gray lamina at 96.0–96.2 cm, together with the layers immediately above this layer, represent predominantly impact ejecta.

We consider the first two alternatives as less likely. The extended sections of clay-rich material probably represent sedimentation during long time intervals (see Thierstein et al., this volume). The bulk of the calcareous microfossils in the 1-m-thick clay-rich section represent Tertiary species (however, reworked Cretaceous fossils are also common; Thierstein et al., this volume). Also the 15-cm-thick laminated interval contains significant amount of Tertiary microfossils. The biological productivity that led to formation of the Tertiary biogenic calcite must have taken place over a long period of time. It seems implausible that new Tertiary species could have evolved and became widely distributed during the short time period while a global dust cloud would have been suspended in the atmosphere. The laminated and the turbated clay-rich intervals possibly formed during time spans of 10^3 – 10^5 yr.

A possibility that must be considered is whether the clay of the 1-m-thick clay-rich zone represents a world-encircling dust cloud related to an extended period of Cretaceous/Tertiary boundary volcanism (e.g., Officer et al., 1987). However, considering the literature about globally distributed Cretaceous/Tertiary boundary clays, no consistent set of hard mineralogical or chemical data favoring the involvement of volcanism in the boundary event has yet been presented. For example, minerals that are typically associated with volcanic ash layers are in general very rare or absent in the Cretaceous/Tertiary boundary layers (Izett and Bohor, 1987; Schmitz, 1988b). In a few cases, on a regional scale, volcanism seems to have played a subordinate role for the formation of the boundary clays (e.g., possibly in Denmark; see Elliot et al., 1989; Schmitz, 1990); however, at any given time volcanism occurs at many places all over the world. Considering the many Cretaceous-Tertiary boundary localities studied, it would be strange if none showed evidence of ongoing volcanic activity.

Most likely, the bulk of the clay in the major part of the 15-cm-thick laminated interval and the 1-m-thick clay-rich interval has a local provenance. An asteroid impact or associated astronomical processes must have triggered some kind of oceanic process that led to clay formation in the marine environment. An understanding of the oceanic process that led to the formation of the marine boundary clays and clay-rich zones would shed further light on the sequence of events that led to extinctions in the marine biosphere.

Whereas the clay in the major part of the clay-rich Cretaceous/Tertiary boundary section in Hole 738C represents with a high degree of certainty predominantly locally derived material, the origin of the clay in the very Ir-rich layer at 96.0–96.2 cm, and in the similarly strongly Ir-enriched layers immediately above is more enigmatic. We have tried to solve this problem by two different approaches to our data for the elements Sc, U, Th, Cs, Hf, and Ta. One approach considers elemental ratios, and the other considers data recalculated on a calcite-free basis. (The different authors of this paper favor different views as to the most reasonable interpretation of our data in this question. The views discussed under the heading "Elemental ratios" reflect mainly those held by B. S. The section "Calcite-free data" reflects the views held by F. A. and H.V.M. The remaining co-authors have not taken a viewpoint as to the chemical arguments presented.)

Elemental ratios

If the bulk of the clay in the dark lamina at 96.0–96.2 cm and in the 1-cm-thick interval immediately above (95–96 cm) has a different provenance than the material higher up in the Cretaceous/Tertiary boundary clay-rich zone, then one would expect that ratios between different elements such as Hf, Ta, Th, U, Cs, and Sc would differ between the levels. None of the elements considered are particularly enriched in meteorites, and there are good reasons to believe that, in the Cretaceous/Tertiary interval of Hole 738C, the elements are primarily associated with the clay phase and not with authigenic or biogenic constituents.

If, for example, the clay in the Ir-rich 95–96.2 cm interval was predominantly made up of altered target rock related to an asteroid impact, this altered target rock would today almost certainly have different Hf/Sc, U/Sc, U/Th, Hf/Ta, Th/Cs, and Cs/Ta, etc., ratios than the locally derived clay higher up. Considering, for example, Sc-normalized ratios for Hf, Ta, Th, U, and Cs, such ratios span more than two to three orders of magnitude in various types of crustal material. The likelihood is very small that an asteroid would strike earth-crust material with the same Sc-normalized concentrations of these elements as the locally derived material at Hole 738C.

The average Sc (10 ppm)-normalized concentrations of Hf, Ta, U, Th, and Cs in the 95–96.2 cm interval respective in the 82–90 cm interval of Section 119-738C-20R-5 are presented in Table 3. The Sc-normalized concentrations of the five elements are almost identical between the two intervals. The very small differences that exist between the two intervals are smaller than the natural variations that occur within the 82–90 cm interval. The Sc-normalized data in Table 3 represent a strong argument that the bulk of the clay of the very Ir-rich 95–96.2 cm interval represents the same kind of locally derived material as the clay in the overlying levels of the Cretaceous/Tertiary boundary clay-rich zone. If one or two of the five considered elements had similar Sc-normalized abundances in the 95–96.2 cm interval as in the 82–90 cm interval, this could have been reconcilable with a target-rock origin of the lower clay; however, the fact that all five elements have similar abundances strongly supports a common origin of the lower and upper clay. Important to consider is

Table 3. Average element concentrations in upper and lower laminated Cretaceous-Tertiary boundary intervals of Section 119-738C-20R-5.

Interval (cm)	Hf (ppm)	Ta (ppm)	U (ppm)	Th (ppm)	Cs (ppm)	Ir (ppb)	Sc (ppm)
Sc (10 ppm)-normalized							
82-90	0.94	0.15	0.61	3.4	0.68	6.6	—
95-96.2	0.95	0.13	0.50	3.3	0.61	15.8	—
Calculated calcite-free							
82-90	3.81	0.61	2.51	13.8	2.79	27.2	40.8
95-96.2	3.01	0.42	1.58	10.4	1.94	50.1	31.6

that from the results displayed in Table 3 it also follows that all other elemental ratios between the elements of concern (e.g., Th/Ta, Sc/Ta, U/Th, Cs/U, etc.) are identical (within the precision of our approach) between the 95-96.2 cm and the 82-90 cm intervals.

Not only the elemental ratios, but also clay mineralogical studies indicate a local origin of the aluminosilicates in the 95-96.2 cm interval. Clay minerals of the dark lamina at 96.0-96.2 cm are indistinguishable from clay minerals in other sections of the laminated Cretaceous/Tertiary boundary interval (Thierstein et al., this volume). Moreover, fine laminations a few centimeters below 96.2 cm suggest that the event (most likely the Cretaceous/Tertiary boundary asteroid impact) that triggered the formation of the laminated clay at Hole 738C may have taken place some time before the formation of the lamina at 96.0-96.2 cm. If the 96.0-96.2 cm or 95-96.2 cm interval represents an ejecta fallout layer it is very difficult to explain why it formed some time after the laminated clay at Hole 738C began to form. Another difficulty is the occurrence of Tertiary foraminifers in the 4-cm-thick interval below the 96.2 cm level (Huber, this volume). It is worth mentioning that the "transition layer" underlying the most Ir-rich layer at Hole 738C is an arrangement similar to that found in unbioturbated Cretaceous/Tertiary boundary clays at Stevns Klint in Denmark, Caravaca in Spain, and Woodside Creek in New Zealand (see Schmitz, 1988b, 1990).

The mixing time of the oceans is a few thousand years (Broecker and Peng, 1982). If abundant extremely fine particulate or dissolved extraterrestrial matter was dispersed in ocean surface water near an asteroidal impact site far away from the Kerguelen Plateau (for example, along the coast of North America, see Schmitz, 1988b, 1990; Kunk et al., 1989), it would take a rather long time before this material reached the Kerguelen Plateau through natural mixing and reworking processes in the ocean. Asteroids probably become completely vaporized upon impact on Earth. The atoms in the asteroid may become ionized, leading to a high susceptibility for the elements to end up in a dissolved state in seawater. The dissolved Ir would sooner or later precipitate and settle on the seafloor. Moreover, atomized and ionized iridium ejected to high altitudes in connection with the asteroid impact may have remained dispersed in the stratosphere for a long time. This Ir would ultimately have been scavenged by stratospheric dust and water vapor. If the 95-96.2 cm interval represents a relatively slow-forming deposit, there would have been sufficient time for seawater-dissolved Ir and extremely fine-particulate Ir-carrying particles to accumulate in the layer.

The oceanic process that led to the formation of locally derived clay at ODP Hole 738C and many other Cretaceous/Tertiary boundary sites worldwide (Schmitz, 1988a, b, 1990) is not understood. Perhaps a large-scale astronomical process, of which the Cretaceous/Tertiary boundary asteroidal impact was only a marginal manifestation, affected the rotation and/or shape of

the Earth. This would have affected global oceanic circulation patterns, sea level, and climate. Turbulence in the oceanic water mass with accompanying clay formation could, perhaps, have resulted from changing tidal conditions, or from a rearrangement of the global water mass in relation to the solid earth.

Calcite-free data

An alternative interpretation (favored by F. A. and H.V.M.) of the origin of the clay in the 96.0-96.2 cm interval and in the immediately overlying intervals is also built on the consideration of abundances of Ta, Hf, U, Th, Sc, and Cs across the Cretaceous/Tertiary boundary clay-rich zone. However, instead of using elemental ratios, F. A. and H.V.M. consider the variations of the elements with their concentrations recalculated to a calcite-free basis (Table 3). Calcite data from Thierstein et al. (this volume; see also Fig. 1) were used, and the whole-rock abundances of the concerned elements were divided by the non-carbonate mass of respective sample.

It follows from Table 3 that the calcite-free abundances of Hf, Ta, Th, U, Sc, and Cs are substantially lower in the 95-96.2 cm interval than in the 82-90 cm interval. This is considered as evidence for the admixture of the clay of the 95-96.2 cm level with a substantial fraction of extraneous material with low concentrations of these five elements.

In the case of Ta, which, according to F. A., is the perhaps most reliable element from which to make these types of deductions, different mass-mixing calculations provide estimates of the amount of exotic material present in the strongly Ir-enriched intervals of the laminated section (see Table 4). Assuming that the extraneous material has a Ta content of 0.00 ppm and that the local detritus at Hole 738C has a Ta concentration of 0.61 ppm (i.e., the average calcite-free Ta concentration of the 82-90 cm interval), the 96.0-96.2 cm level would contain 37% extraneous material. Assuming the other extreme, that the Ta content of the extraneous material is 0.39 ppm (i.e., the calcite-free Ta content measured in the 96.0-96.2 cm interval), results in the 96.0-96.2 cm interval containing 100% extraneous material. Because Ta abundances of clays near 0.00 ppm are very rare and those of 0.4 ppm are much more common, the second scenario presented in Table 4 is more probable than the first. According to F. A. and H.V.M., at least 37% and more likely 90%-100% of the mass of the clay in the 96.0-96.2 cm interval has a different provenance (impact-ejecta fallout material) than the locally derived clay higher up in the section.

Additional aspects on the Hf, Ta, Sc, Cs, U, and Th data

Depending on choice of data processing technique it is possible to reach different conclusions as to the origin of the Ir-rich dark lamina in Hole 738C. Both techniques discussed are attached with problems. For example, the lower calcite-free abundances of Hf, Ta, Sc, Cs, U, and Th in the dark lamina com-

Table 4. Possible abundance of extraneous component in the clay fraction of Section 119-738C-20R-5.

Sample interval (cm)	Extraneous material	
	if Ta content = 0.00 ppm (%)	if Ta content = 0.39 ± 0.02 ppm (%)
90-91	8 ± 8	20 ± 20
91-92	4 ± 9	12 ± 22
92-93	9 ± 9	25 ± 17
93-94	20 ± 8	56 ± 16
94-95	20 ± 8	56 ± 13
95-96	27 ± 7	74 ± 13
96.0-96.2	37 ± 6	100

pared with intervals higher up, could be due to an unknown component other than calcite or impact-related material that dilutes the sediment. Possible components could be opaline silica and/or crystalline and interstitial water. The elements show on average a factor of 0.73 lower concentrations in the 95–96.2 cm interval lamina compared with the 82–90 cm interval. This means that the whole-rock sediment of the lower interval may be diluted by about 8% of material with insignificant concentrations of the considered elements.

The precision of the calcite measurements is critical for our interpretations. For a sediment with 90% calcite, an error of 2% (a too high value) in the calcite determination would cause an error of 25% for the calculated calcite-free data. The calcite concentrations used in our study were determined by leaching the sediment with acetic-acid (10%) and weighing the residue (see Thierstein et al., this volume). Some of the weight difference between a leached and an unleached sample may be due to loss of other constituents than calcite. Such components may be sea salt from pore water, gypsum, and anhydrite. A sediment with 30% pore water before drying will contain about 1.5% sea salt after drying. The water-binding capacity of the sediment samples may also determine weight differences between leached and original samples. Acetic-acid leaching and weighing is a rather rough method to determine the calcite content of a sediment. The reproducibility of duplicate carbonate analyses of our samples was better than 0.5% (Thierstein et al., this volume), however, this does not tell us anything about the accuracy of the analyses.

As regards the elemental ratios there are also problems. One potential flaw that may underlie our reasoning is that the clay minerals at ODP Hole 738C have exchanged trace elements with the surrounding pore water to that extent that all original differences between various precursor materials have been smudged out. In general, however, trace element patterns are more stable and more indicative of precursor materials than, for example, clay mineralogy and major element chemistry. Another possibility is that a significant fraction of the trace elements of concern, contrary to expectations, actually occur in authigenic minerals and not the clay phase. This would make the whole picture more complicated. We are, for example, puzzled by the fact that calculated calcite-free concentrations of Sc in our samples are as high as 32–41 ppm. Most clays contain 15–20 ppm Sc. Did the clay precursor at the Kerguelen Plateau contain anomalously high Sc concentrations, or is there another explanation? Whereas the chemical data presented here may give at least indications about the origin of the clay fraction of the dark lamina at 96.0–96.2 cm, more detailed studies of, for example, Sr isotopes, shocked quartz and chromite occurrences, roundness of quartz grains, calcite content, and major element chemistry are necessary in order to finally resolve the origin of the dark lamina.

SUMMARY

The Cretaceous/Tertiary boundary in Hole 738C is characterized by a 1-m-thick zone of sediment with enhanced clay concentrations relative to background. The basal 15 cm of this clay-rich zone is finely laminated, and in the layers a few centimeters above the base of the laminated interval Ir concentrations are as high as 18 ppb (whole rock). This Ir most likely has the same origin as the Ir found in enhanced concentrations at many Cretaceous/Tertiary boundary sites all over the world. Detailed studies of such Ir anomalies in sediments deposited in nonmarine environments in North America indicate that the Ir derives from an extraterrestrial bolide that impacted the Earth.

The bulk of the clay in the major part of the 1-m-thick clay-rich zone (including the interval from at least the middle of the laminated interval to the top of the clay-rich zone) most likely has a local provenance and formed over a long time interval.

Possibly an asteroid impact or, more likely, an associated large-scale astronomical process catalyzed an undefined oceanic process leading to formation of clay-rich sediments in the marine environment all over the world. Two possibilities appear to exist regarding the strongly Ir-enriched layers a few centimeters above the base of the laminated interval. One possibility is that the clay of the layers predominantly represents locally derived material and that the Ir enhancements represent an admixture of the layers with a small fraction of previously atomized or ionized extraterrestrial matter. Some of this Ir may have been dissolved in seawater before it reached the seafloor. The second possibility is that the very Ir-rich layers primarily are made up of fallout material (asteroidal matter and target rock) related to an impact-ejected, sun-blocking global dust cloud. Further isotopic and mineralogical studies of the boundary section may throw additional light on the origin of the Ir-rich clay.

ACKNOWLEDGMENTS

This work was supported by the Office of Basic Energy Sciences of the U.S. Department of Energy (Contract no. DE-ACO3-76SF00098) and by the U.S. National Aeronautics and Space Program (Contract no. A-59508C). Financial support to B. S. was provided by the Swedish Natural Science Foundation and the Blancefloor-Ludovici Boncompagni, Born Bildt, Foundation. The late L. W. Alvarez generously invited B. S. to work on this and related projects at the Lawrence Berkeley Laboratory. Construction of the Iridium Coincidence Spectrometer was made possible primarily by grants from the M. J. Murdock Charitable Trust in Vancouver, Washington. We thank F. T. Kyte and C. J. Orth for helpful reviews. Photographic slides of the core sections studied were kindly provided by J. Barron.

REFERENCES

- Alvarez, L. W., Alvarez, W., Asaro, F., and Michel, H. V., 1980. Extraterrestrial cause for the Cretaceous-Tertiary extinction. *Science*, 208: 1095–1108.
- Alvarez, W., Alvarez, L. W., Asaro, F., and Michel, H. V., 1982. Iridium anomaly approximately synchronous with terminal Eocene extinctions. *Science*, 216:868–888.
- , 1984. The end of the Cretaceous: sharp boundary or gradual transition. *Science*, 223:1183–1186.
- Boström, K., Joensuu, D., Moore, C., Boström, B., Dalziel, M., and Horowitz, A., 1973. Geochemistry of barium in pelagic sediments. *Lithos*, 6:159–174.
- Boström, K., Moore, C., and Joensuu, O., 1979. Biological matter as a source for Cenozoic deep sea sediments in the equatorial Pacific. *Ambio, Spec. Rept.*, 6:11–17.
- Broecker, W. S., and Peng, T.-H., 1982. *Tracers in the Sea*: Palisades, NY (Eldigio Press).
- Church, T. M., 1979. Marine barite. In Burns, R. G. (Ed.), *Reviews in Mineralogy* (Vol. 6). Mineral Soc. Am., 175–209.
- Dehairs, F., Chesselet, R., and Jedwab, J., 1980. Discrete suspended particles of barite and the barium cycle in the open ocean. *Earth Planet. Sci. Lett.*, 49:528–550.
- Elderfield, H., and Pagett, R., 1986. Rare earth elements in ichthyoliths: variations with redox conditions and depositional environment. *Sci. Total Environ.*, 49:175–197.
- Elliot, W. C., Aronsson, J. L., Millard, H. T., Jr., and Gierlowski-Kordesch, E., 1989. The origin of the clay minerals at the Cretaceous/Tertiary boundary in Denmark. *Geol. Soc. Am. Bull.*, 101:702–710.
- Goldberg, E. D., and Arrhenius, G.O.S., 1958. Chemistry of Pacific pelagic sediments. *Geochim. Cosmochim. Acta*, 13:153–212.
- Haskin, L. A., Haskin, M. A., Frey, F. A., and Wildeman, T. R., 1968. Relative and absolute terrestrial abundances of the rare earths. In Ahrens, L. H. (Ed.), *Origin and Distribution of the Elements*: New York (Pergamon), 889–912.
- Izett, G. A., 1988. *The Cretaceous-Tertiary (K-T) Interval Raton Basin Colorado and New Mexico and Its Content of Shock-Metamorphosed Minerals: Implications Concerning the K-T Boundary Impact-Extinction Theory*: Open-File Rept. U.S. Geol. Surv., 87-606.

- Izett, G. A., and Bohor, B. F., 1987. Comment on "Dynamic deformation of volcanic ejecta from the Toba Caldera: possible relevance to Cretaceous/Tertiary boundary phenomena." *Geology*, 15:90.
- Kastner, M., Asaro, F., Michel, H. V., Alvarez, W., and Alvarez, L. W., 1984. The precursor of the Cretaceous-Tertiary boundary clays at Stevns Klint, Denmark, and DSDP Hole 465A. *Science*, 226:137-143.
- Krauskopf, K. B., 1979. *Introduction To Geochemistry* (2nd ed.): New York (McGraw-Hill).
- Kunk, M. J., Izett, G. A., Haugerud, R. A., and Sutter, J. F., 1989. ^{40}Ar - ^{39}Ar dating of the Manson impact structure: a Cretaceous-Tertiary boundary crater candidate. *Science*, 244:1565-1568.
- Margolis, S. V., Mount, J. F., Doehne, E., Showers, W., and Ward, P., 1987. The Cretaceous/Tertiary boundary carbon and oxygen isotope stratigraphy, diagenesis, and paleoceanography at Zumaya, Spain. *Paleoceanography*, 2:361-377.
- Michel, H. V., Asaro, F., Alvarez, W., and Alvarez, L. W., 1983. Abundance profiles of iridium and other elements near the Cretaceous/Tertiary boundary in Hole 516F of Deep Sea Drilling Project Leg 72. In Barker, P. F., Carlson, R. L., Johnson, D. A., et al., *Init. Repts. DSDP, 72*: Washington (U.S. Government Printing Office), 931-936.
- _____, 1990. Geochemical studies of the Cretaceous-Tertiary boundary in ODP Holes 689B and 690C. In Barker, P. F., Kennett, J. P., et al., *Proc. ODP, Sci. Results*, 113: College Station, TX (Ocean Drilling Program), 159-168.
- Officer, C. B., Hallam, A., Drake, C. L., and Devine J. D., 1987. Late Cretaceous and paroxysmal Cretaceous/Tertiary extinctions. *Nature*, 326:143-149.
- Oudin, E., and Cocherie, A., 1988. Fish debris record the hydrothermal activity in the Atlantis II deep sediments (Red Sea). *Geochim. Cosmochim. Acta*, 52:177-184.
- Perlman, I., and Asaro, F., 1969. Pottery analysis by neutron activation. *Archaeometry*, 11:21-52.
- _____, 1971. Pottery analysis by neutron activation. In Brill, R. H. (Ed.), *Science and Archaeology*: Cambridge, MA (MIT Press), 182-195.
- Schmitz, B., 1987. Barium, equatorial high-productivity, and the northward wandering of the Indian continent. *Paleoceanography*, 2:63-77.
- _____, 1988a. Marine and continental Cretaceous/Tertiary boundary clays compared. In *Global Catastrophes in Earth History*. LPI Contrib., 673:164-165. (Abstract)
- _____, 1988b. Origin of microlayering in worldwide distributed Ir-rich marine Cretaceous/Tertiary boundary clays. *Geology*, 16:1068-1072.
- _____, 1990. Replies on comments by F. T. Kyte, B. F. Bohor, and D. M. Triplehorn on "Origin of microlayering in worldwide distributed Ir-rich marine Cretaceous/Tertiary boundary clays." *Geology*, 18:87-94.
- Schmitz, B., Andersson, P., and Dahl, J., 1988. Iridium, sulfur isotopes and rare earth elements in the Cretaceous-Tertiary boundary clay at Stevns Klint, Denmark. *Geochim. Cosmochim. Acta*, 52:229-236.
- Smit, J., and Romein, A.J.T., 1985. A sequence of events across the Cretaceous-Tertiary boundary. *Earth Planet. Sci. Lett.* 74:155-170.
- Taylor, S. R., and McLennan, S. M., 1988. The significance of the rare earths in geochemistry and cosmochemistry. In Gschneidner, K. A., Jr., and Eyring, L. (Eds.), *Handbook on the Physics and Chemistry of Rare Earth*, Vol. 11: Amsterdam (Elsevier), 485-578.
- Tschudy, R. H., and Tschudy, B. D., 1986. Extinction and survival of plant life following the Cretaceous/Tertiary boundary event, Western Interior, North America. *Geology*, 14:667-670.
- Wedepohl, K. H., 1969. *Handbook of Geochemistry*: Berlin (Springer Verlag).
- Wright, J., Schrader, H., and Holser, W. T., 1987. Paleoredox variations in ancient oceans recorded by rare earth elements in fossil apatite. *Geochim. Cosmochim. Acta*, 51:631-644.
- Zachos, J. C., and Arthur, M. A., 1986. Paleoceanography of the Cretaceous/Tertiary boundary event: inferences from stable isotopic and other data. *Paleoceanography*, 1:5-26.

Date of initial receipt: 9 October 1989

Date of acceptance: 30 May 1990

Ms 119B-166